Progress in Additive Manufacturing
https://doi.org/10.1007/s40964-022-00346-y

FULL RESEARCH ARTICLE

Prediction of tensile strength in fused deposition modeling process using artificial neural network and fuzzy logic

Amanuel Diriba Tura[1] · Hirpa G. Lemu[2] · Hana Beyene Mamo[1] · A. Johnson Santhosh[1]

Received: 17 March 2022 / Accepted: 15 September 2022

Abstract
Fused deposition modeling is a modern rapid prototyping technique that is used for swiftly replicating concept modeling, physical modeling, and end-of-line manufacture. Precision parameter selection is crucial for generating high-quality products with excellent mechanical properties, such as tensile strength. This study looked at three essential process variables: infill density, extruder temperature, and print speed. The relationship between these parameters and tensile strength of printed polylactic acid components was investigated. Artificial neural network (ANN) and Fuzzy logic (FL) method are utilized to develop a prediction model. The test samples have been printed using a 3D forge Dreamer II FDM printing machine. In Minitab software, the response surface design of the Box–Behnken technique with 15 experimental sets was used to organize the trials. The results revealed that extruder temperature and print speed had a minor impact on tensile strength; however, infill density has a large impact. The ANN and FL models all predicted tensile strength with a high degree of accuracy, with maximum absolute percentage errors of 2.21%, and 3.29%, respectively. The model and the experimental data were found to be in good agreement, according to the findings. Furthermore, when compared to FL modeling, ANN models with arithmetical value indices were the best predictive model.

Keywords Fused deposition modeling · Tensile strength · Artificial neural network · Fuzzy model

1 Introduction

Additive manufacturing (AM) is a new technique that creates a product directly from a computer-aided design (CAD) model using a layer-based production approach. Flexible thermoplastic filament is extruded via a heated nozzle to construct components in fused deposition modeling (FDM), which is one of numerous 3D printing procedures. ABS, PLA, polycarbonate, Ultem, PEEK, and fiber-reinforced thermoplastics are among the thermoplastics and reinforced thermoplastic materials that may be produced with FDM. In a variety of industries, including as automotive, aviation, and medicine, FDM-produced components are progressively substituting traditional components [1–5]. The process variables and their settings have a significant impact on the mechanical characteristics of FDM produced components. As a result, increasing the mechanical features of printed components requires analyzing the effects of input elements and anticipating results by using appropriate process settings [6–8].

Several scholarly studies were conducted to create a prediction model and examine the impact of printing parameters on the mechanical qualities of FDM components. For instance, Pazhamannil and Govindan [9] built an artificial neural network to predict the tensile strength of FDM printed objects at various nozzle temperatures, layer thicknesses, and infill rates. Using 33 trials and result data, Manoharan et al. [10] used ANN to develop mathematical models for evaluating the tensile strength of FDM made PLA components. The actual tensile strength results were compared to the anticipated values using the RSM, ANN, and ANOVA

✉ A. Johnson Santhosh
johnsonsanthosh@gmail.com; Johnson.antony@ju.edu.et

Amanuel Diriba Tura
diriba.amanuel@ju.edu.et

Hirpa G. Lemu
Hirpa.g.lemu@uis.no

Hana Beyene Mamo
hanicho2102@gmail.com

1 Faculty of Mechanical Engineering, Jimma Institute of Technology Jimma University, Jimma, Ethiopia

2 Faculty of Science and Technology, University of Stavanger, Stavanger, Norway

findings. According to Enemuoh et al. [11], infill density has a significant impact on the tensile strength of the FDM component, followed by layer thickness, print speed, and infill pattern. Response surface approach is used by Srinivasan et al. [12] to predict and optimize the impact of process parameters (infill density, infill pattern, and layer thickness) on tensile strength in FDM-produced ABS components.

Gebisa and Lemu [13] investigated the impact of process factors such as air gap, raster angle, raster width, contour width, and contour number on the tensile properties of components manufactured using the FDM technique and using ULTEM 9085 polymeric material. The raster angle, according to their research, has a significant influence on tensile properties. Hsueh et al. [14] studied how FDM process factors affected the mechanical characteristics of PLA and PETG materials. The results reveal that when the printing temperature rises, the PLA and PETG materials' mechanical performance (tension, compression, and bending) increase. Furthermore, when manufacturing speed increases, the PLA material's mechanical behavior improves, whereas the mechanical properties of the PETG material decrease. Experimental testing and finite element analysis were utilized by Patil et al. [15] to evaluate the tensile and flexural strength of FDM printed PLA components. Rayegani and Onwubolu [16] use differential evolution (DE) and the group method for data handling (GMDH) to predict and improve the relationship between FDM component tensile strength and process parameters (part alignment, raster angle, raster width, and air gap). The infill density and printing pattern had a substantial impact on the tensile strength of polylactic acid FDM printed components, according to Zhou et al. [17].

Byberg et al. [18] investigated the effects of layer alignment and build direction on the mechanical (tensile, compression, and flexural) characteristics of ULTEM 9085 thermoplastic. According to their results, the layer orientations and manufacturing directions have a significant impact on the characteristics of this polymer. The contribution of process variables (layer height and printing speed) on the mechanical characteristics of 3D-printed ABS composite was studied by Christiyan et al. [19]. They observed that the material's best tensile and flexural strength came from a combination of low manufacturing speed and thin layer height. Hsueh et al. [20] investigated the impact of printing temperature and filling % on the mechanical parameters of FDM printed PLA components using tension and Shore D hardness examinations. Raising the filling proportion or printing temperature, according to their research, may significantly improve the material's tensile Young's modulus, ultimate strength, elongation, and Shore hardness.

Pre-processing variables, according to the literature, have a considerable impact on the mechanical properties of FDM-produced components. It was also critical to look at the combined effect of FDM parameters on the mechanical characteristics of the components that were created. As a result, three crucial pre-processing factors (infill density, extruder temperature, and printing speed) for obtaining high tensile strength product have been selected. Furthermore, the ANN, and Fl approach were used to develop predicted data.

Table 1 The specification of the Flash Forge Guider II 3D printer

Name	Guider II
Number of extruder	1
Print technology	Fused filament fabrication (FFF)
Build volume	280 × 250 × 300 mm
Layer resolution	0.05–0.4 mm
Build accuracy	± 0.2 mm
Positioning accuracy	Z axis 0.0025 mm; XY axis 0.011 mm
Filament diameter	1.75 mm (± 0.07)
Nozzle diameter	0.4 mm
Nozzle temperature	210–250 °C
Platform temperature	0–120 °C
Print speed	10–200 mm/s

Table 2 The specification of the PLA printing materials

Properties	Specification
Color	Bumblebee yellow
Wire diameter (mm)	1.75 ± 0.05
Recommended printing temperature (°C)	185–205
Recommended printing speed (mm/s)	30–90
Extrusion temperature (°C)	190–210
Bed platform temperature (°C)	25–80
Density (g/cm^3)	1.25

2 Materials and methods

2.1 3D printer and materials

A Flash Forge Guider II 3D printer was used to create the specimens in this study. The build envelope of the printer measures 280 × 250 × 300 mm^3 and can generate components with 0.2 mm accuracy. The 3D printer's characteristics are shown in Table 1. The study employed polylactic acid (PLA) since it is a strong thermoplastic and a typical FDM material. PLA is a biodegradable polymer filament with a higher tensile strength than most existing polymers but lower ductility [21]. The mechanical properties of the printing materials are shown in Table 2.

2.2 Experimental design

According to the literature, process parameters have a significant influence on the mechanical qualities of FDM-produced components. Therefore, examining the combined effects of FDM settings on the mechanical qualities of the generated components was critical. As a result, three process variables were chosen as research input variables: infill density, extruder temperature, and printing speed with three levels. The values of each element were adjusted according to machine manufacturer recommendations. Table 3 lists the process parameters and their ranges that were explored during this study. The other parameters are kept at their default settings. Table 4 shows the response surface design of the Box–Behnken approach, which was used in a total of 15 tests.

2.3 Specimen fabrication

The test specimen was 3D modeled using CATIA V5 software, as per the criteria. The stereo lithography (STL) format is used to save the CAD file, which is then transferred to the slicer for separation into the needed number of layers.

Table 3 Process parameters and their range for experiments

S. no.	Process parameters	Units	Levels		
			− 1	0	1
1	Infill density	%	20	60	100
2	Extruder temp	°C	190	200	210
3	Print speed	mm/s	50	100	150

Using flash print slicing software, the printing settings are also included. The slicer then transforms the STL file to a G-code file, which the printers use to begin layer-by-layer fabrication of the specimen. The ASTM D638- I standard [22] was used to create the tensile test specimens. The samples prepared according to this standard have dimensions of $165 \times 13 \times 3.2$ mm in length, width, and thickness.

2.4 Experimental procedure

The UNITEK-94100 universal testing machine (UTM) (Dhara Agency, Gujarat, India) was used to assess the tensile strength of PLA specimens conditioned according to the ASTM D638 standard. The top grip moved at a constant pace of 2.5 mm/min, with a maximum load of 100 kN and a 5 Hz signal sampling rate. The built-in program recorded the ultimate tensile strength, elongation, and force load data. When the specimen exceeds 2.5% elongation or breaks, the test is terminated. The experimental results of the tensile strength are presented in Table 4.

2.5 Artificial neural network (ANN) modeling

ANN is computer programs that are designed after the organic neural networks that make up a brain. ANN is used to model nonlinear conditions and predict output values using training data. An ANN structure network consists of input and output layers, as well as multiple hidden layer neurons [23]. The neural network has three layers: an input layer, an output (or target) layer, and a hidden layer in between. Between the input and output layers is a layer known as the hidden layer, where

Table 4 Categorical Box–Behnken experimental design matrix and measured responses

Standard order	Run order	Input parameters			Output response
		Infill density (%)	Extruder temp. (°C)	Print speed (mm/s)	UTS (MPa)
13	1	60	210	150	34.79
14	2	60	210	50	32.62
6	3	100	200	150	43.39
11	4	60	200	100	36.67
4	5	100	210	100	45.27
10	6	20	200	150	33.00
8	7	100	200	50	41.00
5	8	100	190	100	43.48
7	9	20	200	50	35.68
1	10	60	200	100	36.81
15	11	20	210	100	36.50
12	12	60	190	150	30.24
9	13	20	190	100	34.84
2	14	60	200	100	36.61
3	15	60	190	50	32.89

artificial neurons receive a series of weighted inputs and generate an output using an activation function. ANN uses samples of data rather than the whole data set available in the system for quick prediction, saving money and time in the process. ANN can easily be replaced by existing data analysis systems [24].

The ANN model was used to train and evaluate data models for 3D printing. MATLAB was used to generate an input layer with three inputs, a hidden layer with feed-forward conditions applied, and a single output layer (Fig. 1). The network was trained using the experimental data from Table 5. The ANN design and learning variables utilized in this study are shown in Fig. 1.

Table 5 Learning parameters designated for ANN

Type of network	Feed-forward neural network
Training function	Train Levenberg–Marquardt(LM)
Adaption learning function	LEARNGD (Gradient descent)
Performance function	Mean square error
Network topology	3-10-1
Transfer function	TANSIG
Number of hidden layers	1
Number of neurons	10
Training method	Back-propagation
Number of epochs	1000

2.6 Fuzzy logic modeling

The idea of modeling parameters when the values are unknown or linguistic variables are used instead of numerical values is known as fuzzy logic. This hypothesis of idea was for the first time developed by Zdeh [25]. Fuzzy modeling is an effective approach for dealing with such challenges in the conditions outlined, especially for anticipating outcomes. There are many other kinds of fuzzy membership functions, such as triangular, trapezoidal, and Gaussian, that may be used with almost any mathematical operator [26, 27]. In the present study, three inputs, namely infill density, extruder temperature, and printing speed are used with one output, i.e., ultimate tensile strength (UTS). The triangle membership function, as described by Eq. (1), explored for these parameters. The fuzzy set A can be seen in this equation, along with the fuzzy number *x*. A(*x*) is the membership function, and the factors *l*, *m*, and *u* signify the lowest, most likely, and major possible rates, respectively.

$$\mu_A(x) = \begin{cases} \frac{(x-l)}{(m-l)}, & l \le x < m, \\ \frac{(u-x)}{(u-m)}, & m < x \le u, \\ 0, & otherwise \end{cases} \tag{1}$$

Figure 2 illustrates the membership functions of all the parameters of this study including the output and inputs of the proposed fuzzy modeling using fuzzy inference system (FIS). For each of the inputs, a three-degree triangular fuzzy membership function with three linguistic standards like L (Low), M (Medium), and h (High) are deliberated. A seven-degree triangle fuzzified function is proposed for the output, with Very Low (VL), Low (L), Low Medium (LM), Medium (M), High Medium (HM), High (H), and Very High (VH) as options. A fuzzy inference system (FIS) is presented to

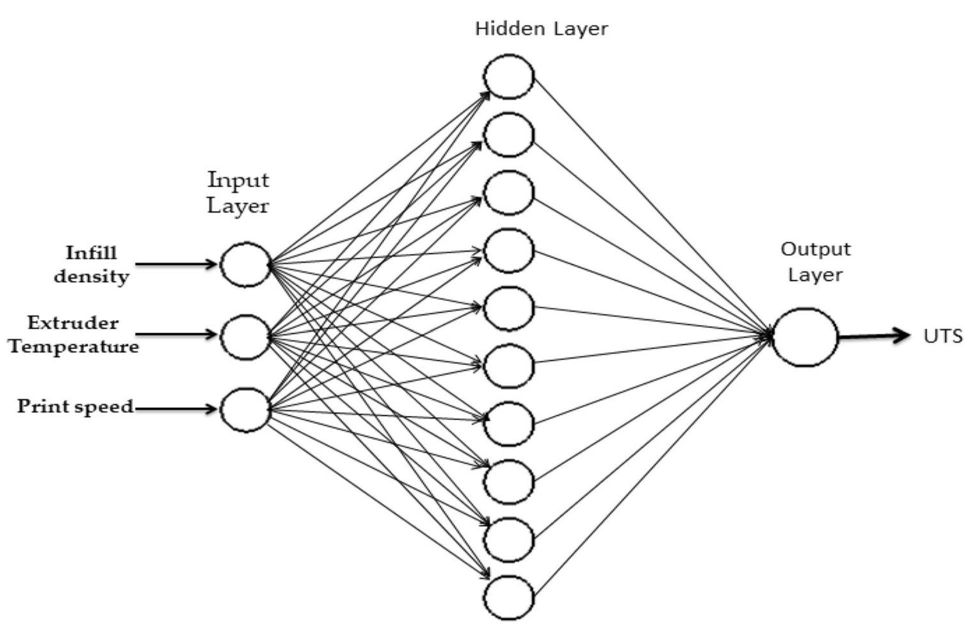

Fig. 1 Structure of the neural network

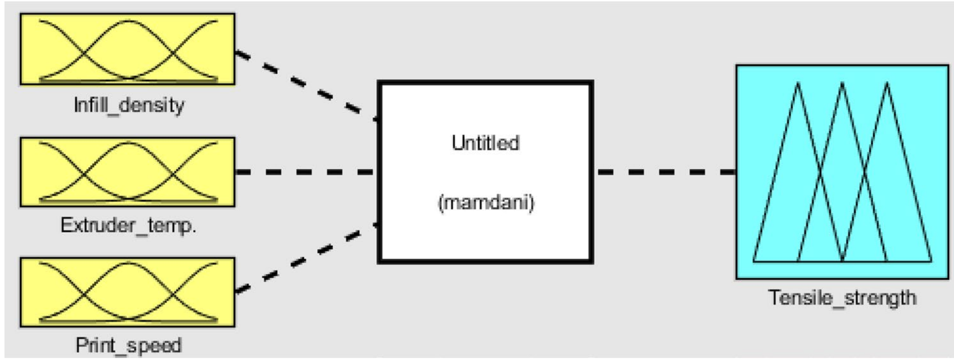

Fig. 2 Layout of the designed Fuzzy Logic

Table 6 Properties of the proposed FIS

FIS type	Mamdani
Inputs; outputs	3; 1
Input membership function	Triangular
Output membership function	Triangular
Weights of rules	1
Number of rules	15
And method	Min
Implication method	Min
Aggregation method	Max
Defuzzification method	Centroid

develop the fuzzy model, and its properties are provided in Table 6.

Figure 3 illustrates the triangular membership functions of all the parameters of this study including the inputs and output of the proposed fuzzy modeling using FIS. In the fuzzy logic modeling, fifteen *If–Then* rules were considered.

3 Results and discussion

3.1 Investigation of effect of process parameters on tensile strength

Analysis of variance (ANOVA) was used to examine the results for tensile characteristics in order to explore the major factors that influence the quality measures. Factors with a very modest probability (Prob > *F* value) less than 0.05 are considered significant in the ANOVA table, whereas factors with a probability (Prob > *F* value) larger than 0.1 are considered inconsequential. Furthermore, larger *F* values and lower *P* values have a greater impact on the performance characteristic derived from designed process parameters. Table 7 shows the ANOVA of each process parameters on ultimate tensile strength of PLA parts. According to the ANOVA results (Table 7), the combinations of infill density and extruder temperature are insignificant factors affecting the final tensile strength of PLA parts.

Figure 4 shows the main effects plot for UTS, which demonstrates the fluctuation of UTS with the inputs. This main effect graph for the average value of UTS shows that the UTS declines with increasing infill density, but then dramatically increases after 60%. Extruder temperature has less effect on UTS, and UTS increases somewhat as extruder temperature rises, but at around 200 °C, it begins to decline slightly. In other circumstances, UTS increased as print speed increases, but at around 100 mm/s, it begins to decrease.

The contour plots showing the influence of each of the two input variables on ultimate tensile strength are shown in Fig. 5a–c. Blue colored zones represent very low and low-level values, green zones show low-medium, medium, and high-medium values, while yellow zones represent high and very high volumes in these graphs. Figure 5a exhibits the impact of infill density (ID) and extruder temperature (ET) on the UTS, and the contour plots in the figure illustrate that higher UTS values were obtained at increased infill density and extruder temperature. Figure 5b depicts the impact of ID and printing speed (PS) on UTS. It can be seen from these interaction graphs that infill density has a considerable impact on UTS, while printing speed has a little impact on UTS. In a similar fashion, the impact of ET and PS on UTS is depicted in Fig. 5c, which shows that greater UTS values were achieved at 100 mm/s printing speed and 200 °C extrudes temperature.

3.2 Results of artificial neural network modeling

When the error, or the difference between the expected and predicted output, is less than a defined upper bound, or when the number of epochs exceeds a specified threshold, the ANN is stopped training. A score near to 1 implies a strong connection, while a value close to 0 shows a random relation. Figure 6 illustrates the 78-iteration regression graphs developed by artificial neural networks. The regression plots obtained reveal that for training, testing, validation, and total data, 0.99901, 1,

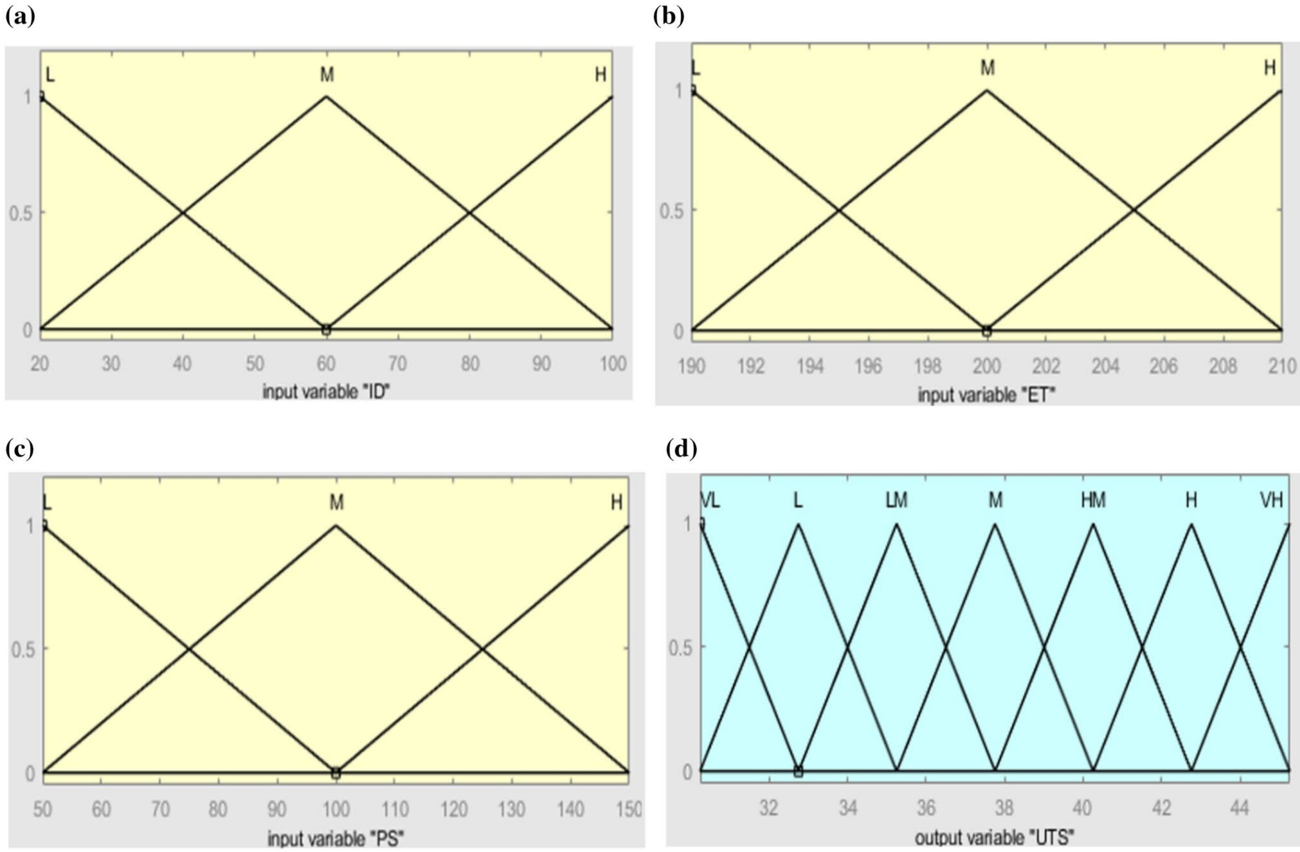

Fig. 3 Triangular MFs of **a** Infill density **b** Extruder temperature **c** Print speed and **d** Tensile strength

Table 7 ANOVA for ultimate tensile strength of PLA parts

Source	DF	Adj SS	Adj MS	*F* value	*P* value	
Regression	9	276.258	30.6954	324.52	0.000	
A	1	1.505	1.5045	15.91	0.010	Significant
B	1	4.581	4.5809	48.43	0.001	Significant
C	1	1.992	1.9921	21.06	0.006	Significant
A*A	1	74.079	74.0785	783.17	0.000	Significant
B*B	1	4.911	4.9114	51.92	0.001	Significant
C*C	1	31.231	31.2310	330.18	0.000	Significant
A*B	1	0.004	0.0042	0.04	0.841	Not Significant
A*C	1	6.426	6.4262	67.94	0.000	Significant
B*C	1	5.808	5.8081	61.40	0.001	Significant
Error	5	0.473	0.0946			
Lack-of-fit	3	0.452	0.1506	14.30	0.066	
Pure error	2	0.021	0.0105			
Total	14	276.731				

A is infill density, B is extruder temperature, and C is print speed

1, and 0.99918, respectively, suggesting the best fitness after repeated training. This indicates that the ANN model's anticipated outcomes appear to be in line with the experimental data. The ANN model worked adequately, as shown in Table 8, with average percentage error of 0.40% from the experimental results, demonstrating its

Fig. 4 Main effect plots of UTS for means with all process parameters

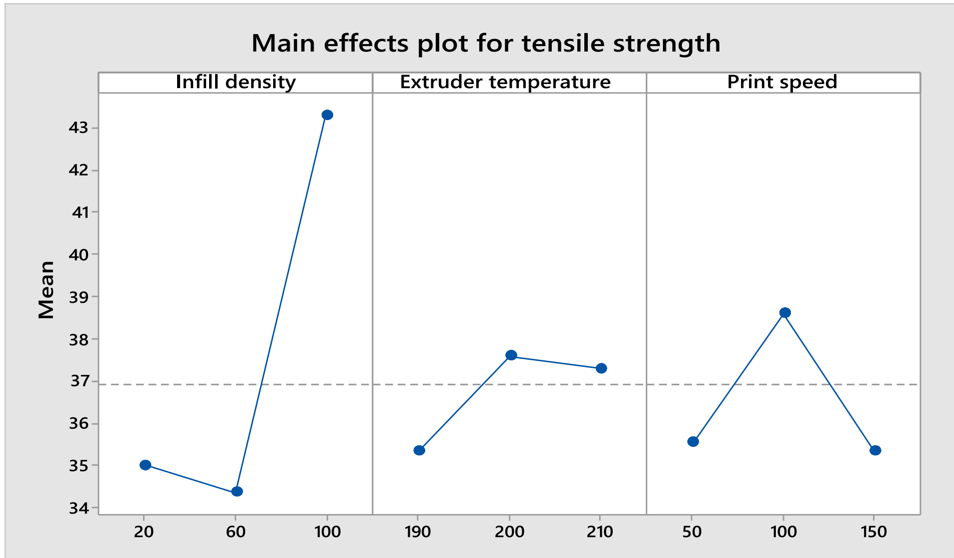

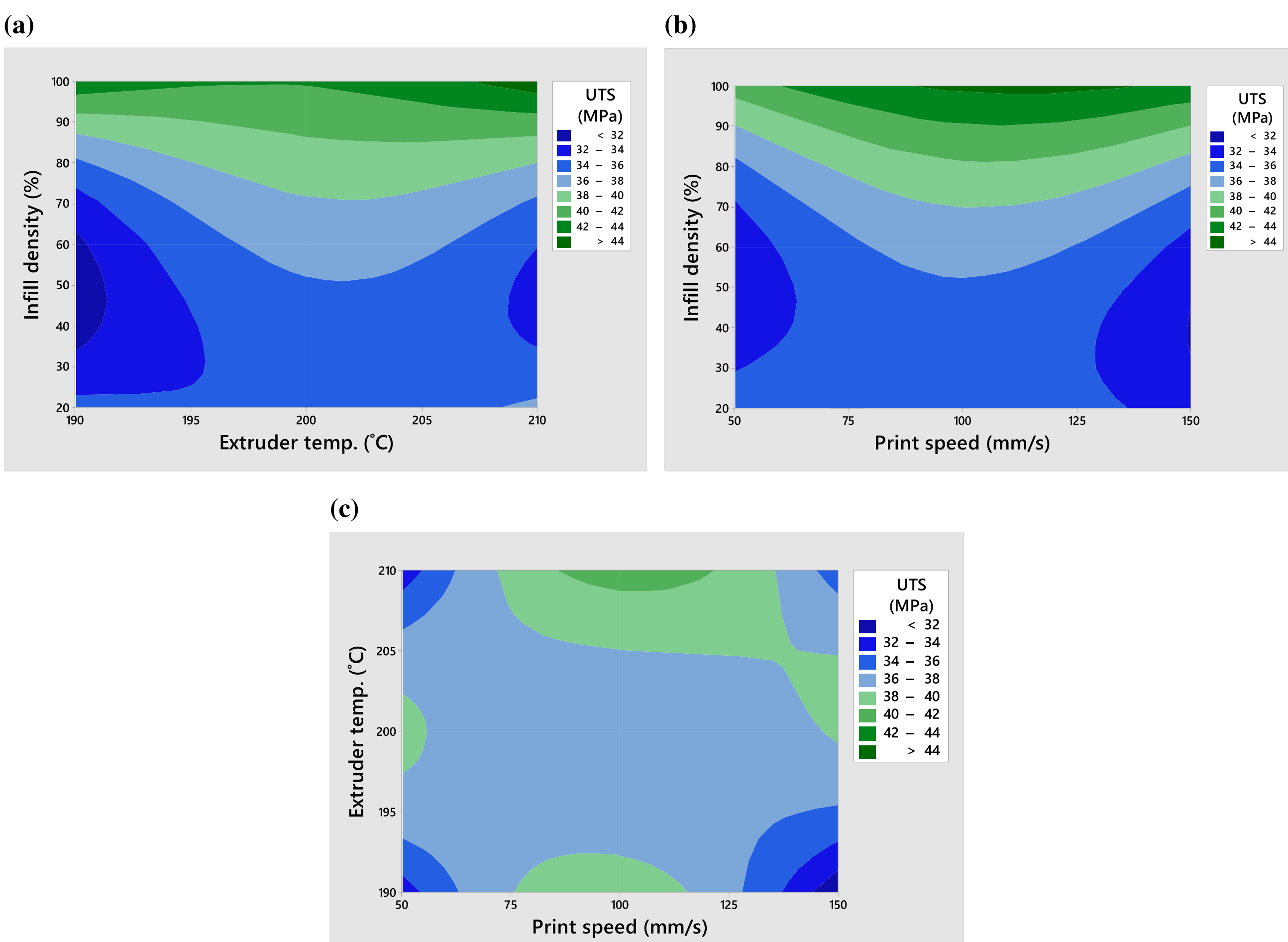

Fig. 5 Contour plots of **a** infill density (ID) and extruder temperature (ET), **b** infill density and printing speed (PS) and **c** extruder temperature and printing speed with ultimate tensile strength

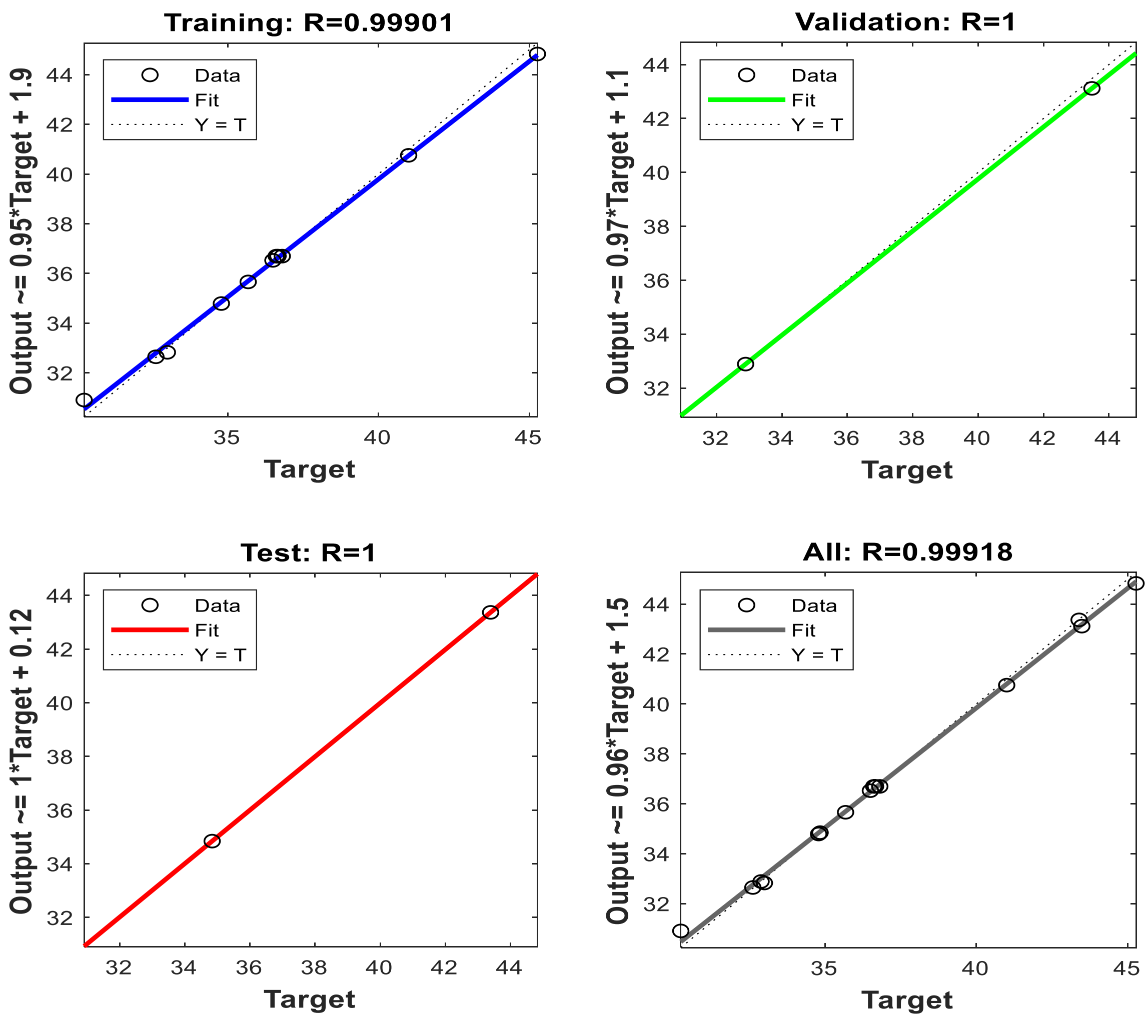

Fig. 6 Regression plots for ultimate tensile strength obtained using artificial neural networks

Table 8 Comparative evaluation of predictive models

Exp. trials	Experimental results of UTS	ANN model		FL model	
		Predicted results	% errors	Predicted results	% errors
4	34.79	34.7898	0.001	35.3	– 1.47
5	32.62	32.6479	– 0.09	32.7	– 0.25
6	43.39	43.3666	0.05	42.8	1.36
7	36.67	36.6974	– 0.07	37.8	– 3.08
8	45.27	44.8277	0.98	44.1	2.58
9	33.00	32.8279	0.52	32.7	0.91
10	41.00	40.752	0.61	40.3	1.71
11	43.48	43.1152	0.83	42.8	1.56
12	35.68	35.6601	0.01	35.3	1.07
13	36.81	36.6974	– 0.31	37.8	– 2.69
14	36.50	36.5263	– 0.07	35.3	3.29
15	30.24	30.9083	– 2.21	31	– 2.51
16	34.84	34.8451	– 0.01	35.3	– 1.32
17	36.61	36.6974	– 0.24	37.8	– 3.25
18	32.89	32.8872	0.01	32.7	0.58
Average percentage error			0.40		1.84

potential for future usage. Sample number 12 exceptionally over predicts with maximum absolute deviation of 2.21%.

3.3 Results of fuzzy logic modeling

Based on the data in Table 6, the MATLAB R2019a program was used to obtain the outcomes of the suggested fuzzy model. Instead of dealing with a fuzzy number using Eq. (2), the FIS output should be defuzzified to offer a number as the final result after modeling. In this equation, x^* is the output crisp number, x_i is the center point of each component, $\mu\ (xi)$ is the ith rule's level, and n is the number of the processed rules in the fuzzy model. After computation using this equation (Eq. (2)), the produced outputs are compared with the experimental results.

$$x^* = \frac{\sum_{i=1}^{n} x_i.\mu(x_i)}{\sum_{i=1}^{n} \mu(x_i)} \quad (2)$$

The fuzzy modeling of the rules is shown in Fig. 7, where the experimental results, fuzzy predicted data from FIS, and the percentage error between each pair of data are given in Table 8. The largest inaccuracy of results given in the table is related to sample number 11, which underpredicts by 3.29%. Such results clearly demonstrate that the fuzzy modeling system is a very effective strategy that can be utilized when there is no precise data for the inputs or when performing the experimental analysis is challenging.

3.4 Comparative evaluation of the predictive models

To compare the ANN, and FL the predictive result and the experimental results of UTS are analyzed by their average percentage error of the responses. Error percentage for ANN, and FL were computed individually by comparing the predicted values with the test results using Eq. (3). The average percentage error of the ANN model was 0.40%, and the FL model was 1.84%, as shown in Table 8. This demonstrates that the ANN model was the most accurate or best predicting model technique. Figure 8 compares the plotted output data from experimental, ANN modeling, and FL modeling.

$$\%Error = \frac{Actual - predicted}{Actual} \times 100 \quad (3)$$

4 Conclusions

Applications of artificial neural networks, and fuzzy logic techniques to predict tensile strength for parts produced from PLA material using fused deposition modeling are proposed in this paper. All of the investigations were carried out using a 15 Box–Behnken response surface design to alter the input parameters at different levels. The relationship between input parameters and output result were studied using analysis of variance and main effect plots. The results of the experiments were used to train and test the developed models. The artificial neural network and fuzzy logic model were all designed using the MATLAB R2019a neural toolbox and

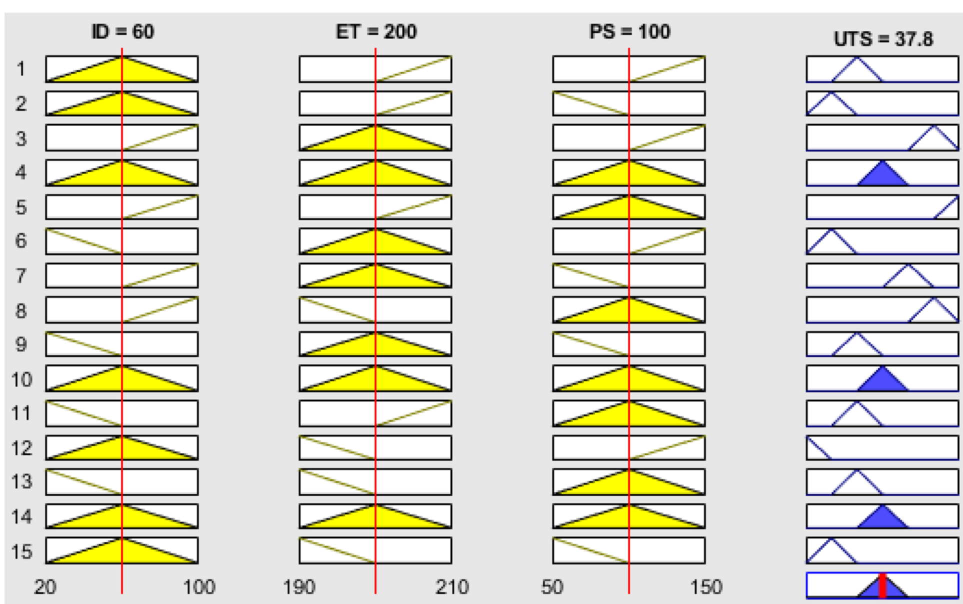

Fig. 7 Rules set for the given data

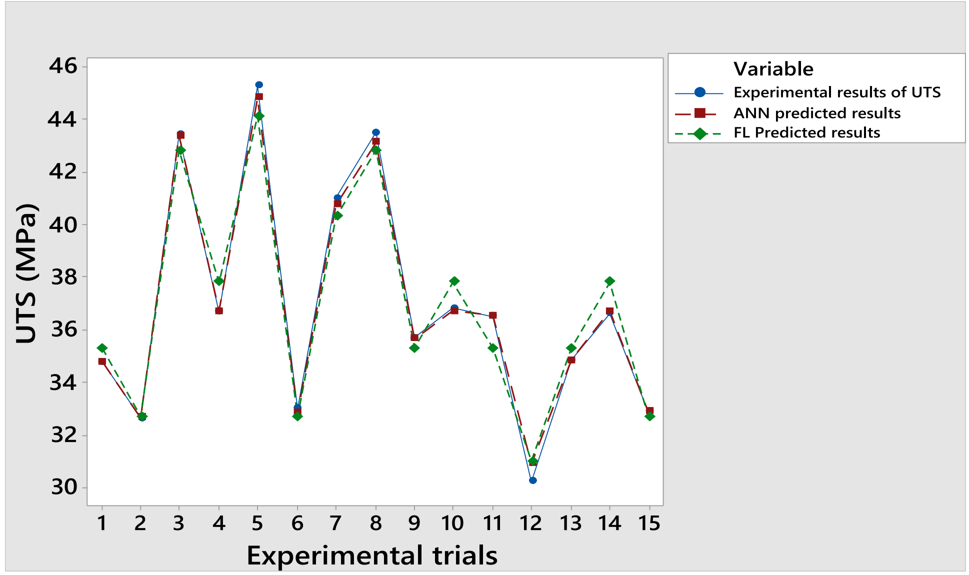

Fig. 8 Comparison of experimental and predicted outputs

fuzzy toolbox, respectively. The models' capability to predict was measured in percentage error. The following findings may be taken from the research:

- According to the ANOVA results, the combinations of infill density and extruder temperature are insignificant factors that affect the ultimate tensile strength of PLA parts.
- Infill density has the greatest impact on ultimate tensile strength while indicates that extruder temperature and printing speed have little effect on UTS, according to the main effect plots.
- According to 3D and contour plots, the highest Ultimate tensile strength were achieved at higher infill density, higher extruder temperature, and printing speed in the center.
- The ANN and FL models can accurately predict tensile strength with average percentage errors of 0.40, and 1.84 respectively.
- The ANN and FL models exhibit a close correlation between expected and experimental outcomes with less than 5% error. When compared to FL modeling, ANN models with arithmetical value indices were likewise the most predictive.

Acknowledgements The authors also acknowledge Jimma Institute of Technology's, Faculty of Mechanical Engineering for providing experimental facilities and financial assistance for this study.

Author contributions ADT and HBM: Conceptualization; ADT and AJS: methodology; ADT: software; ADT and HGL: validation; ADT and HBM: formal analysis; ADT and HBM: investigation; ADT and HGL: resources; ADT and HGL: data curation; ADT: writing—original draft preparation; HGL: writing—review and editing; HGL: visualization; AJS and HGL: supervision; HBM: project administration; HGL: funding acquisition. All authors have read and agreed to the published version of the manuscript.

Data availability Not applicable.

Declarations

Conflicts of interest The authors declare no conflict of interest.

References

1. Gebisa AW, Lemu HG (2018) Investigating effects of Fused-deposition modeling (FDM) processing parameters on flexural properties of ULTEM 9085 using designed experiment. Materials (Basel) 11:1–23
2. Peterson AM (2019) Review of acrylonitrile butadiene styrene in fused filament fabrication: a plastics engineering-focused perspective. Addit Manuf 27:363–371
3. Tura AD, Mamo HB, Jelila YD, Lemu HG (2021) Experimental investigation and ANN prediction for part quality improvement of fused deposition modeling parts. IOP Conf Ser Mater Sci Eng. https://doi.org/10.1088/1757-899X/1201/1/012031/meta
4. Motaparti KP, Taylor G, Leu MC, Chandrashekhara K, Castle J, Matlack M (2017) Experimental investigation of effects of build parameters on flexural properties in fused deposition modelling parts. Virtual Phys Prototyp 2017(12):1–14
5. Dong G, Wijaya G, Tang Y, Zhao YF (2018) Optimizing process parameters of fused deposition modeling by Taguchi method for the fabrication of lattice structures. Addit Manuf 19:62–72
6. LaleganiDezaki M, Ariffin MK, Serjouei A, Zolfagharian A, Hatami S, Bodaghi M (2021) Influence of infill patterns generated by CAD and FDM 3D printer on surface roughness and tensile strength properties. Appl Sci 11(16):7272
7. Hsueh MH, Lai CJ, Chung CF, Wang SH, Huang WC, Pan CY et al (2021) Effect of printing parameters on the tensile properties of 3d-printed polylactic acid (Pla) based on fused deposition modeling. Polymers (Basel) 13(14):2387

8. Algarni M, Ghazali S (2021) Comparative study of the sensitivity of pla, abs, peek, and petg's mechanical properties to fdm printing process parameters. Curr Comput-Aided Drug Des 11(8):995
9. Pazhamannil RV, Govindan P, Sooraj P (2019) Prediction of the tensile strength of polylactic acid fused deposition models using artificial neural network technique. Mater Today Proc 46(18):9187–9193
10. Manoharan K, Chockalingam K, Ram SS (2020) Prediction of tensile strength in fused deposition modeling process using artificial neural network technique. AIP Conf Proc 2311(1):080012
11. Enemuoh EU, Duginski S, Feyen C, Menta VG (2021) Effect of process parameters on energy consumption, physical, and mechanical properties of fused deposition modeling. Polymers (Basel) 13(15):2406
12. Srinivasan R, Pridhar T, Ramprasath LS, Charan NS, Ruban W (2020) Prediction of tensile strength in FDM printed ABS parts using response surface methodology (RSM). Mater Today Proc [Internet] 27:1827–1832
13. Gebisa AW, Lemu HG (2019) Influence of 3D printing FDM process parameters on tensile property of ultem 9085. Procedia Manuf 30:33–338
14. Hsueh MH, Lai CJ, Wang SH, Zeng YS, Hsieh CH, Pan CY et al (2021) Effect of printing parameters on the thermal and mechanical properties of 3d-printed pla and petg, using fused deposition modeling. Polymers (Basel) 13(11):1758
15. Patil C, Sonawane PD, Naik M, Thakur DG (2020) Finite element analysis of flexural test of additively manufactured components fabricated by fused deposition modelling. AIP Conf Proc. https://doi.org/10.1063/5.0034306
16. Rayegani F, Onwubolu GC (2014) Fused deposition modelling (fdm) process parameter prediction and optimization using group method for data handling (gmdh) and differential evolution (de). Int J Adv Manuf Technol 73:509–519
17. Zhou X, Hsieh SJ, Ting CC (2018) Modelling and estimation of tensile behaviour of polylactic acid parts manufactured by fused deposition modelling using finite element analysis and knowledge-based library. Virtual Phys Prototyp 13:177–190
18. Byberg KI, Gebisa AW, Lemu HG (2018) Mechanical properties of ULTEM 9085 material processed by fused deposition modeling. Polym Test 72:335–347
19. Christiyan KGJ, Chandrasekhar U, Venkateswarlu K (2016) A study on the influence of process parameters on the Mechanical Properties of 3D printed ABS composite. IOP Conf Ser Mater Sci Eng. https://doi.org/10.1088/1757-899X/114/1/012109
20. Hsueh MH, Lai CJ, Liu KY, Chung CF, Wang SH, Pan CY et al (2021) Effects of printing temperature and filling percentage on the mechanical behavior of fused deposition molding technology components for 3d printing. Polymers (Basel) 13(17):2910
21. Boschetto A, Giordano V, Veniali F (2013) Surface roughness prediction in fused deposition modelling by neural networks. Int J Adv Manuf Technol 67:2727–2742
22. ASTM D638-03 Standard Test Method for Tensile Properties of Plastics. https://www.astm.org/d0638-03.html
23. Santhosh AJ, Tura AD, Jiregna IT, Gemechu WF, Ashok N, Ponnusamy M (2021) Optimization of CNC turning parameters using face centred CCD approach in RSM and ANN-genetic algorithm for AISI 4340 alloy steel. Results Eng 11:100251
24. Mahmood MA, Visan AI, Ristoscu C, Mihailescu IN (2021) Artificial neural network algorithms for 3D printing. Materials (Basel) 14(1):163
25. Zadeh LA (1999) Fuzzy sets as a basis for a theory of possibility. Fuzzy Sets Syst 100:9–34
26 Ouellet V, Mocq J, El Adlouni S-E, Krause S (2021) Improve performance and robustness of knowledge-based FUZZY LOGIC habitat models. Environ Model Softw [Internet] 144:105138
27. Basic A, Peko I, Krolo J, Bagavac P (2021) Fuzzy logic modeling of ultimate tensile strength and cost in fused deposition modeling process of additive manufacturing. In: International Conference Mechanical Technologies and Structural Materials, pp 1–10